

Forensic Investigation of A Subway Tunnel Construction Failure

W. F. Lee¹, C. C. Wang², K. Ishihara³, R. N. Hwang⁴

¹Ground Master Construction Ltd. Co., Taipei, Taiwan

²Department of Civil Engineering and Geomatics, Cheng Shiu University, Kaohsiung, Taiwan

³Chuo University, Tokyo, Japan

⁴Moh & Associates, Inc., New Taipei City, Taiwan

Email: ccw@gcloud.csu.edu.tw

ABSTRACT: In this paper, the forensic evidences and investigation of a subway tunnel construction failure occurred in Kaohsiung, Taiwan are presented. The studied construction failure occurred during a cross passage excavation of a shield tunnel construction work of the Kaohsiung Mass Rapid Transit System, and resulted in severe tunnel collapse and extensive ground failure that even reached to ground surface 30m above the tunnel depth. Valuable photo images obtained during and post event, as well as results of special geophysical testing methods were presented and compared to verify proposed failure scenario. Information presented in this paper is hoped to be helpful to improve engineers' knowledge for preventing similar construction risks.

KEYWORDS: Subway, Shield Tunnel, Cross passage, Resistivity Image Profiling Method

1. INTRODUCTION

On 4th of December 2005, a severe construction failure occurred during a cross passage excavation work of the Kaohsiung Mass Rapid Transit System (KMRT). This construction failure resulted in the collapse of 100m long twin shield tunnels and extensive ground failures that even reached to ground surface 30m above the tunnel depth. Forensic investigation on this incident was firstly conducted by collecting valuable photo images taken during emergency remediation. Moreover, excavation conducted after retrofit works were also conducted to recover remains of damaged structures. Proposed failure scenarios could be examined via such solid visual evidences, especially the timeline of failure development. In addition to collect photo images, borehole probing and the resistivity image profiling testing methods with designed testing schemes were conducted to investigate condition of ground failure. Both 2D surface and 3D resistivity image profiling (RIP) methods were successfully adopted in this investigation to identify the problematic local soil condition, scopes of ground failure and the damages of tunnels. This investigation work was in an effort to justify the possible failure causes as well as to evaluate the effectiveness of the applied retrofit work.

In this paper, forensic evidences such as photos taken during the emergency remediation and investigation excavation, as well as

results of forensic investigation tests conducted are presented in detail and analyzed. Proposed failure scenario is then verified. Work presented in this case study is in a hope to serve as an example and reference to the peer engineers in the field of underground construction, as well as to improve engineers' knowledge for preventing similar construction risks.

2. SITE CONDITIONS

The plan and side view of the tunnel are shown in Figure 1. It is to be noted that there was a vehicle underpass just above the two subway tunnels. The twin tunnels were constructed by the shield tunnel boring machines (STBM) which can advance by rotating a large steel disk equipped with cutting blades, while the main body of the boring machine is protected inside the shield. Figure 2 shows the plan view of the failure site. The soil profiles at the locations BO29 and BO30 shown in Figure 2 are indicated in Figure 3, where it can be seen that the deposits comprise predominantly of silty sand with occasional layers of low-plasticity clay (CL) to a depth of 40m. The SPT blow count values, as shown, increase with depth and have values of 20 to 30 at the depth where the sump of cross passage for water collection was constructed (Ishihara and Lee, 2008b).

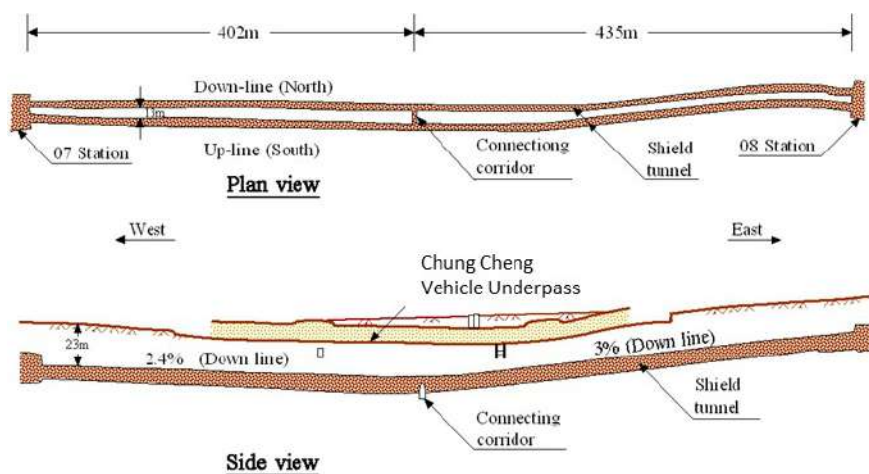


Figure 1 Plan and side views of the studied tunnel site (Ishihara and Lee, 2008)

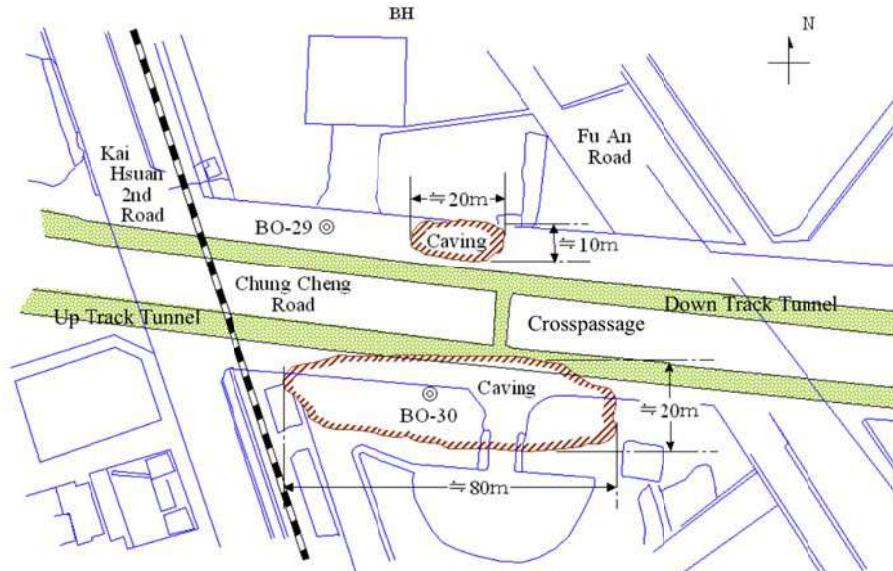


Figure 2 Schematic drawing of the failure site in plan view (Ishihara and Lee, 2008)

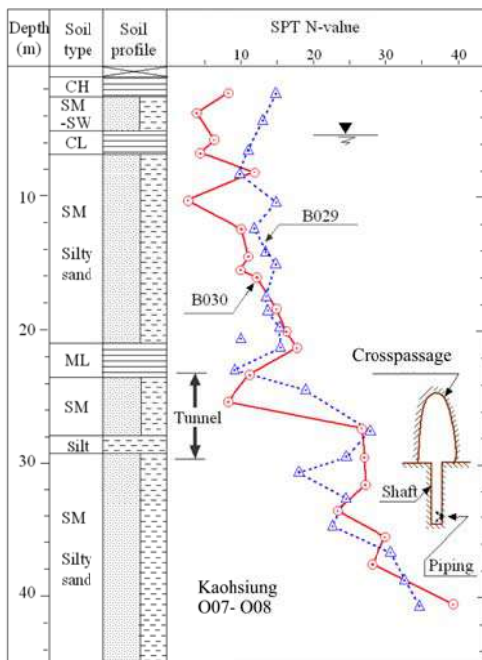


Figure 3 Soil profile of the studied site, before failure (Ishihara and Lee, 2008)

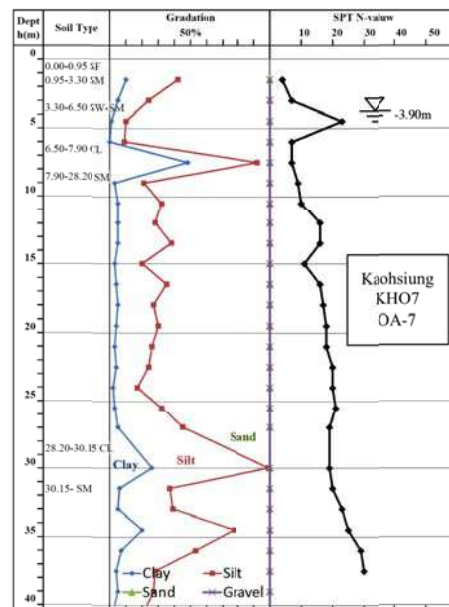


Figure 4 Typical soil profile with gradation data at the site after collapse

Figure 4 also shows a typical soil profile of the studied site after failure with gradation characteristics. As shown in the figure, silty sand deposit at the studied site contains 20% to 35% fines with no plasticity. This silty sand deposit was later studied and confirmed as very sensitive to internal erosion and disturbance (Chen 2012). Ground water table of the studied site is closed to 2~3m below the ground surface. The hydrostatic pressure at the depth where construction failure occurred is over 2.7 kg/cm². Prior to the crosspassage excavation work, soil surrounding the excavation area where the failed crosspassage was located had been stabilized by means of the jet grouting for the purposes of both strengthening the soil and providing water tightness.

3. THE ACCIDENT

The subway was under construction in the central part of Kaohsiung in year 2002 to 2008. Upon finishing the tunnel construction connecting O7 and O8 Stations (Figure 5) by the method of earth-balanced shield tunneling, the crosspassage connecting the up-track and the down-track tunnels was constructed by means of the so-called the NATM method involving open excavation with the help of steel truss support and grout injection. Then, a vertical shaft 3.3m in diameter was excavated to provide a sump for water collection in the middle of the crosspassage in open dry conditions with pre-injected grout protection in the surrounding soil and the support of the H-shaped circular steel beams installed soon after each excavation stage.

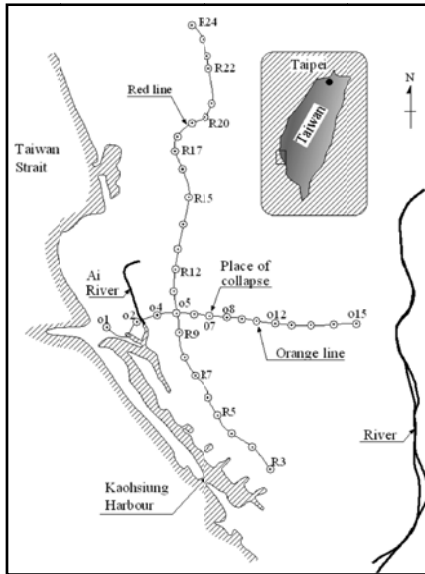


Figure 5 Kaohsiung MRT system and location of the studied site (after Ishihara and Lee, 2008).

In the afternoon of December 4th 2005, when the sump excavation reached a level 4.95m from the floor of the crosspassage, a chunk of wet soil tumbled out from the southern wall of the sump at the bottom around 3:30pm. The small collapse was followed by steadily increased outflow of mud water as shown in Figure 6. At the beginning of the seepage, sand bags and shotcrete were adopted in an effort to stop the flow. However, the amount of water increased with time despite more dry cement and coagulating agents were dumped into the sump. At 4:50pm, water inside the sump started to whirl turbulently showing the signs of collapse of the side wall of the sump. The top cap of the sump was then sealed with anchor bolts, more sand bags, and vertical posts as shown in Figure 7. At 6:00pm, collapse of the sump led to the undermining of the already completed shield tunnels. Water started to spit out between ring lining segments, and chunks of concrete were found to be detached from the edge of ring segments of the shield tunnels (Figure 8). At 6:30pm dislocation of the ring lining segments was clearly identified (Figure 9) and all engineers and workers were forced to evacuate. At 9:30pm nearly 6 hours after the occurrence of the incident, ground above the up-track (south side) tunnel started to settle by 200mm to 250mm. The settlement area soon developed into a big sinkhole within a very short time as depicted in Figure 10, and ruptured several lifeline pipes including two tap water mains of 300mm and 600mm in diameters (Figure 11). By the morning of December 5th, the sinkhole developed to a size of 80m in length and 20m in width (Figure 12). In the meantime, another ground collapse in a size of 20m long and 10m wide was quickly developed on the north side where the down-track tunnel sit below (Figure 13). These two huge cave-ins on the ground surface led to the threat of large scale collapses of the shield tunnels and the crosspassage. These ground cave-ins were finally backfilled and stabilized near the midnight on December 5th, over 30 hours efforts. In addition to the ground failures, the existing vehicle underpass above the failed tunnels was also found to have been seriously damaged by the accident (Figure 14).

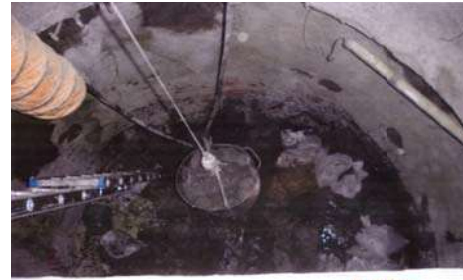


Figure 6 Muddy water started to flow into the bottom of the sump (4:15pm, December 4th, 2005)



Figure 7 Effort made to seal the top of the sump (5:23pm, December 4th, 2005)



Figure 8 Concrete chunks detached from the ring segments of the up-track tunnel (6:30pm, December 4th, 2005)



Figure 9 Serious water inflow and dislocation of lining segments inside the up-track tunnel (6:50pm, December 4th, 2005)



Figure 10 Sinkhole appeared on the ground above the up-track tunnel (10:05pm, December 4th, 2005)



Figure 11 Rupture of the water main (morning of December 5th, 2005)



Figure 12 The large sinkhole on the south side and emergency backfill works in progress (daytime of December 5th, 2005)

4. IMMEDIATE RETROFIT WORK

The first stage of immediate retrofit work mainly focused on backfilling the sinkholes. A total volume of 12,000m³ sand and aggregates, 2,326m³ concrete, as well as 1,150 bags of dry cement,

were dumped from ground surface to fill the sinkholes developed from the deep seated tunnel failures within two days. In addition to backfilling works, remediation grouting and curtain grouting were also applied from both the north and the south boundaries of the vehicle underpass trying to stabilize the existing underground structures and to further confine damaged ground. Figure 15 shows the layout and the total injection volume of grout in cubic meters for the immediate work. In the meantime, four concrete walls sandwiched with sand bags were also constructed at tunnel portals (both up-track and down-track) of O7 and O8 Stations in an effort to retain debris from flowing into the adjacent station areas, as shown in Figure 16. Moreover, in order to stabilize the seriously disturbed ground, water were injected into the tunnels after completion of these retaining walls. This measure was in an attempt to maintain hydrostatic condition of ground, especially at the depth of damaged tunnels. The wall construction and water injecting process was in operation for about seven days before the targeted stable ground water table was reached and maintained (TCRI, 2006). While the retrofit work was in process, ground water table was closely monitored by automatic piezometers installed at different depths at different locations. In addition, settlement survey was conducted on a hourly basis to monitor ground surface settlement closely. Both the settlement and the ground water table measurements were adopted as vital information for safety monitoring and effectiveness of the retrofit works.



Figure 13 the sinkhole development on the north side above the down track tunnel (4:30pm, December 5th, 2005)



(a)



(b)

Figure 14 Damaged vehicle underpass

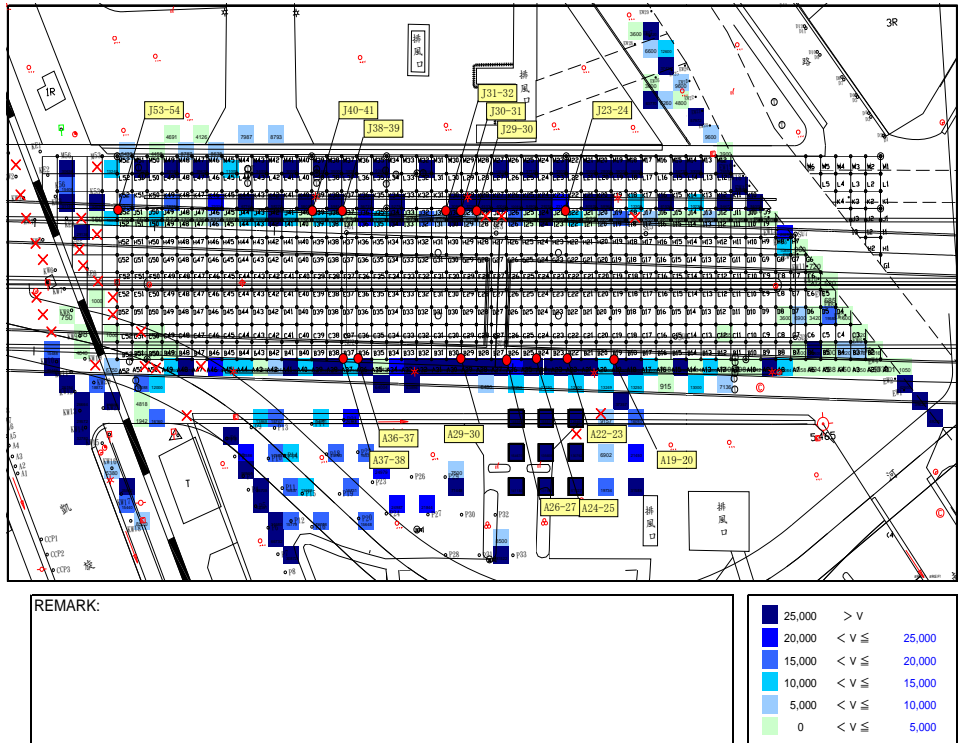


Figure 15 Layout and total volume of grout applied (after TCRI, 2006)



Figure 16 Construction of double layer wall at O7 station side

5. FAILURE INVESTIGATION

5.1 Borehole Probing

Failure investigation was first conducted by drilling boreholes along the original tunnel alignments. The drilling rod was lowered down to the failed ground in an attempt to reach the pre-casted ring segments of the shield tunnel lining. This borehole probing method was used as a direct inspection measure to assess the damaged condition of the shield tunnels and to estimate the length of collapsed and distorted tunnel portions. Borehole probing results of both the up-track and the down-track tunnels are shown in Figure 17 (Lee and Ishihara, 2008b). The cross passage where the incident occurred was located between mileages 0+495m to 0+500m. As shown in the figure, the section between mileages 0+465m to 0+520m of the up-track tunnel had collapsed due to the failure and could not be located by the probing rod. Near 120 meters of the up-track tunnel was seriously dislocated. For the down-track tunnel at

the south of the failed cross passage, the section between mileages 0+475m to 0+515m had collapsed and was out of reach by the probing rod. Similar to the up-track tunnel, near 100 meters of down-track tunnel was seriously disrupted. The result of this borehole probing revealed that ground failure might have destroyed the crosspassage and have destructed nearly 120 meters long up-track and down-track shield tunnels.

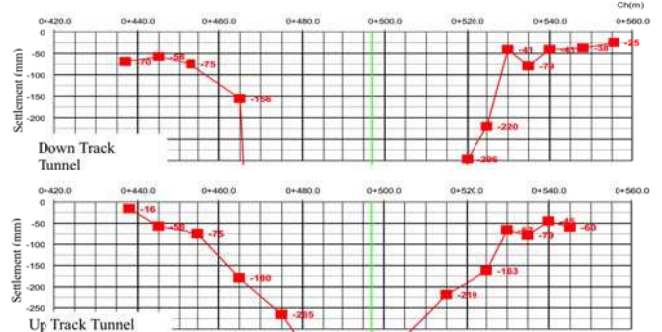


Figure 17 Borehole probing results of the up-track and down-track tunnels

5.2 Resistivity Image Profiling Test

In order to further identify the condition and the extent of ground failure, Resistivity Image Profiling (RIP) test was adopted. RIP was mostly used in investigating geological structures or ground water condition prior to this investigation. RIP has advantages in investigating ground water distribution, geological structures and soil profiles over a large area by measuring electrical resistivity distribution over the target soil deposits or underground space. It was modified to be capable of examining underground structures and complicated ground conditions such as seriously disturbed soil layer and injected grout material (TCRI, 2006). In this forensic study, 2D multiple cross-section and 3D stereo RIP testing were both performed to investigate the ground condition and the damage

to the underground structures. Electrical currents were introduced into the target area by setting up layers of electrical circuits. Resistivity values at specific locations could then be measured by specially arranged sensors installed on ground surface or in boreholes. Figure 18 shows the equipment used and Figure 19 shows probing posts at ground surface used to record resistivity for 2D RIP tests. Figure 20 shows in-hole resistivity sensors before inserting into the boreholes. Measurements of resistivity at specific locations were then used as known boundary conditions and input values of nodes of the analytical models to calculate the resistivity field of the target area.



Figure 18 RIP Testing equipment



Figure 19 Probing posts for 2D RIP tests at ground surface



Figure 20 In-hole resistivity sensors for 3D RIP tests

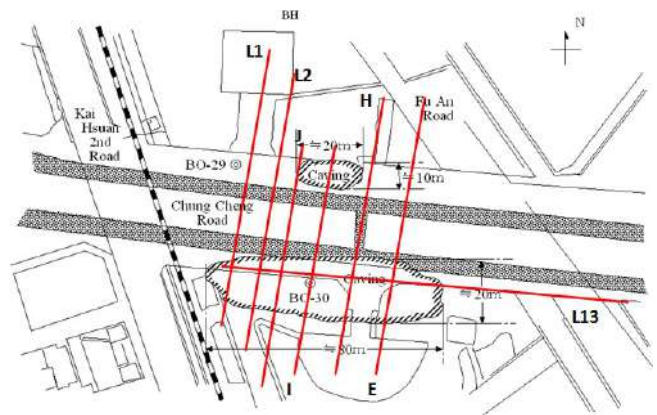
The site was grouted extensively to stabilize the ground prior to excavation. Large numbers of sand bags and lean concrete were dumped into sinkholes to stabilize the disturbed ground after the incident. Underground conditions were fairly complicated when the

RIP surveys were conducted. Optimization of sensor layouts and calibrations of the analytical models were the most challenging issues of this forensic RIP testing (Lee and Ishihara, 2008a). Figure 21(a) shows the layout of the 2D RIP testing. As depicted in the figure, total four longitudinal (east-west direction) and nine transverse (north-south direction) survey lines were conducted in an attempt to cover the damaged area. Moreover, Figure 22 shows the top view and the cross section schematic drawings of the 3D RIP testing. Total six boreholes were drilled to a depth of 40m. This 3D RIP survey was in an effort to assess the damage condition of the cross passage and the up-track shield tunnel.

Figure 23 shows the results of 2D RIP test along the selected survey lines marked in Figure 21(b). In these figures, Calibrated values of resistivity are scaled on the right to each profile. As shown in the image profiles, cold colours, from green to deep blue, represent material with relative low resistivity such as disturbed ground with high ground water content or voids. On the contrary, warm colours, from yellow, orange, to red and brown, represent material with relative high resistivity such as dense soil, injected grouts or concrete. In this case, images obtained by the 2D RIP test tend to be slightly distorted upward because only ground surface probing posts were installed to record response resistivity (Lee and Ishihara, 2008a). However, resistivity profiles shown in Figure 23 still clearly indicate that the area in between the vehicle underpass and the cross passage were in serious distressed condition. Profiles L2, H, and E, identify that ground in between the vehicle underpass and the cross passage in south contained high water content and in a loose state at the time of testing. Similar ground condition was also observed in the ground under the sinkhole on the north as shown in Profiles L1, L2, I, and J. In addition, ground failure area on the south where the up-track tunnel was located was found to be more serious than that on the north where the down-track tunnel is.



(a)



(b)

Figure 21 Layout of 2D RIP tests

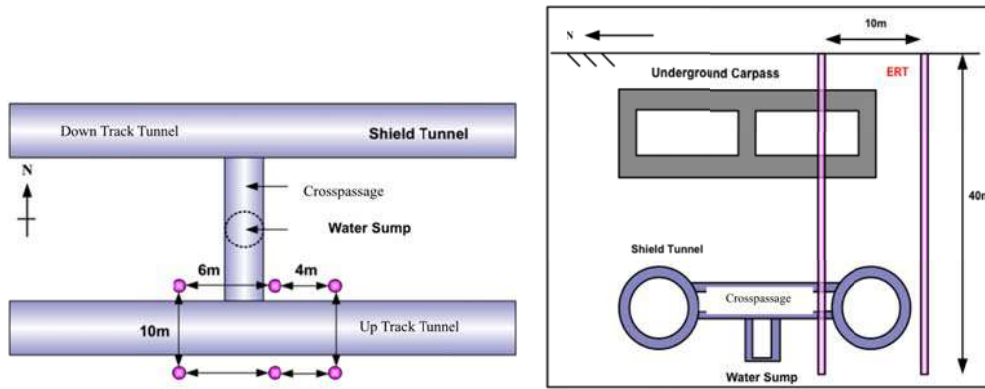


Figure 22 Schematic drawings of 3D RIP tests, (a) overlook view, and (b) cross section view

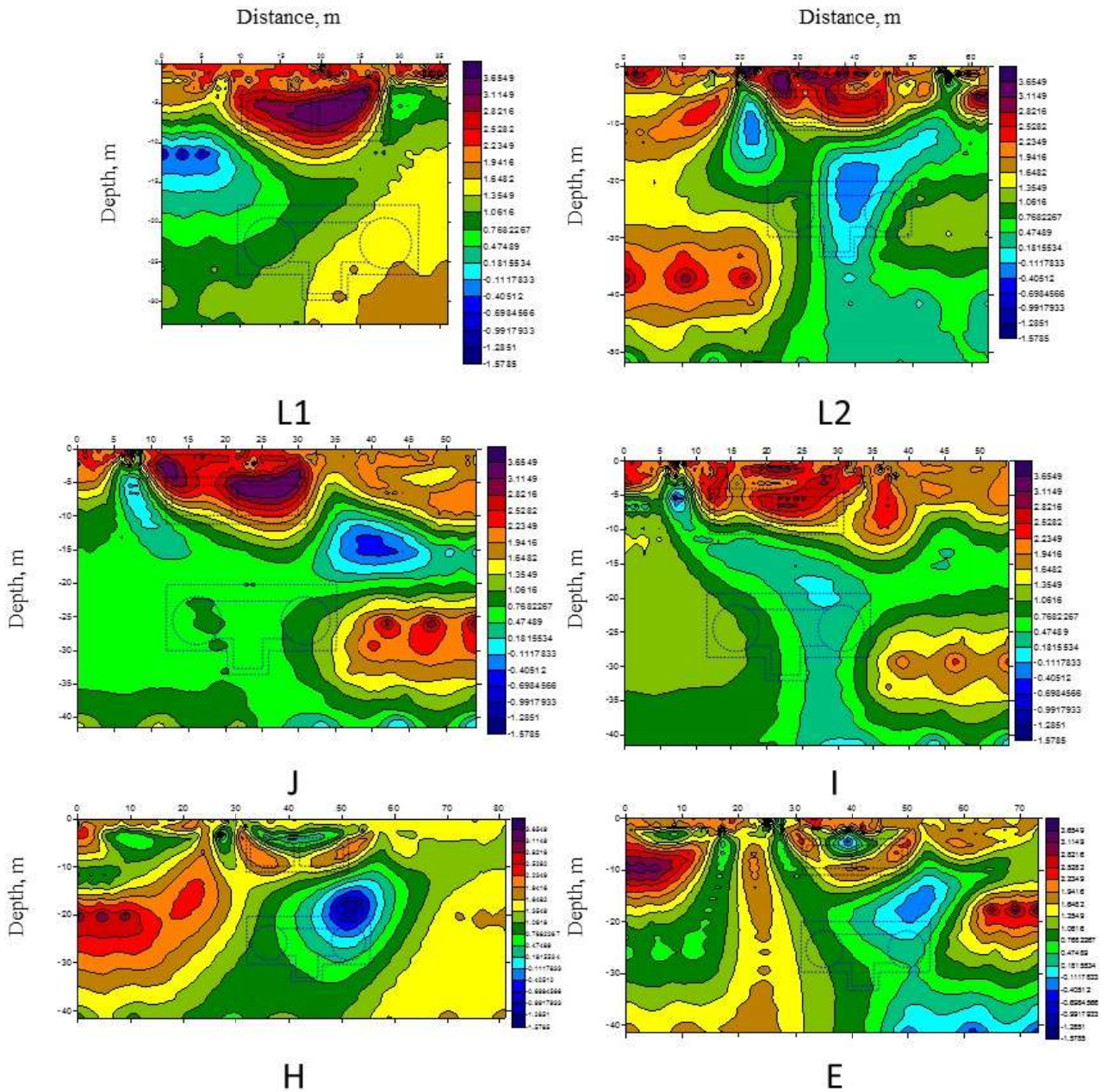


Figure 23 Results of 2D RIP tests

The 2D RIP results also indicated that damaged areas were larger than two sinkholes appearing at ground surface, and further verified the results of borehole probing that near 120m long tunnels in both directions were destroyed by the piping ground. At the locations of profiles L2, H, and E, which were the east and the west boundaries of the soil improvement work for the damaged cross passage, soil beneath the subway tunnels was also found to be severely agitated by possible soil piping or boiling failures. As shown in these image profiles, the shapes of the agitated soil layers are in funnel shapes. This observation indicates that ground failure was initiated at bottom of water sump and then spread upward through the up-track tunnel first to cause large sinkhole on ground surface. Ground failure then migrated to the soil surrounding the down-track tunnel to cause another sinkhole on December 5th, the second day of the accident. Moreover, no clear image of the cross passage or soil improvement block installed before tunnel construction was found in 2D RIP results; this indicates that the cross passage and the shield tunnels attached to it should have been all broken by the huge soil piping pressure. The 2D RIP results also show that immediate remediation and grout treatments had effectively reached the perimeter of the ground failure to possibly stabilize the ground, as the warm colour areas shown in profiles L2, J, I, H, and E.

Figure 24 shows the results of the 3D RIP test. As the results of 3D investigation contained fairly complicated stereo information, images shown in the figure have been processed by carefully differentiating assorted materials underground. The light green or blue portion shown in the figure indicates the most of jet grout material applied prior to the construction of the cross passage and the shield tunnels. Reinforced concrete portions of shield tunnels and the cross passage are probably in bright green to yellowish colour. The exposed steel truss and rebar of the cross passage are in orange to red colours with least electrical resistivity. As shown in Figure 24, the integrity of the shield tunnel and the crosspassage was barely observed. The east portion of the shield tunnel was found to have an offset of at least 1m from the cross passage, and the west portion of the shield tunnel was found to be out of shape with an offset over 2m. There was very low resistivity response in both images indicating that the cross passage might have been seriously damaged to expose steel truss components. The results of 3D RIP test denote that piping failure induced from the water sump had probably destroyed the connections of the shield tunnel to the cross passage. The results of both 2D and 3D RIP tests have further verified the results of borehole probing shown in Figure 17. Moreover, it has provided visualization images describing the failure extent and the actual ground condition. This information is valuable for both forensic investigation as well as retrofit design.

6. FAILURE SCENARIO

Ishihara and Lee (2008b) first proposed the failure hypothesis of the studied incident (Figure 25) based on the investigation data including workmen testimonies, emergency retrofit work records, as well as the forensic testing results presented in this paper. They described that the failure started from the bottom of the water sump highly likely via a vertical piping crack (Ishihara and Lee, 2008). The invasive hydraulic pressure near 300kPa caused by such a piping failure forced debris to flow into the crosspassage from the collapsed water sump. In the early stage of failure, the jet-grouting block installed for crosspassage construction was fairly strong; it was not broken until the hydraulic pressure caused by piping and flown-in debris had ripped off the ring lining segments of the shield tunnels outside such a jet-grouting block. Ground failure was enlarged when the debris flowed into the tunnels and created large voids underground. The failed ground was in a state near liquefaction due to the high hydraulic pressure and strong downward seepage. The shattered ground soon expanded upward to ground surface forming a huge sinkhole above the up-track tunnel on the south and widely spread to the down-track tunnel on the north

creating similar failure. The vehicle underpass sitting above was thus damaged by distressed ground underneath and all ground as depicted in Figure 25 (Ishihara and Lee, 2008). Moreover, Figures 26 and 27 show the wreckages of the cross passage and the shield tunnel excavated during the retrofit works. As shown in Figure 26, the cross passage inclined to the south and sunk over 2m at the edge connecting to the shield tunnels. The shotcrete lining and the inner truss of the cross passage was found to have been severely broken by the debris flown in. Figure 27 shows clearly that the ring lining segments of the shield tunnel had been ripped off and sunk as revealed in the investigation using borehole drilling and RIP tests. Where the cross passage connecting to the two shield tunnels had the most serious settlement and thus damages included dislocation and collapse to lining segments of the shield tunnel as shown in Figure 27. The proposed failure scenario was further verified by such forensic recovery work.

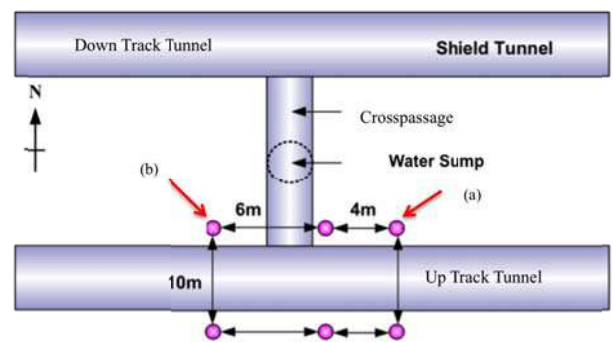
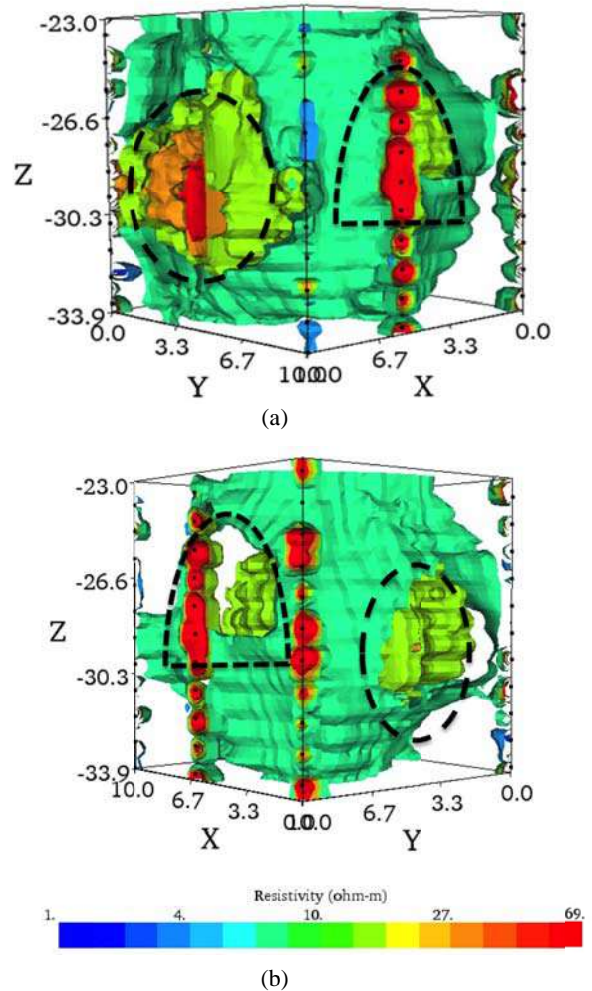


Figure 24 Results of 3D RIP tests

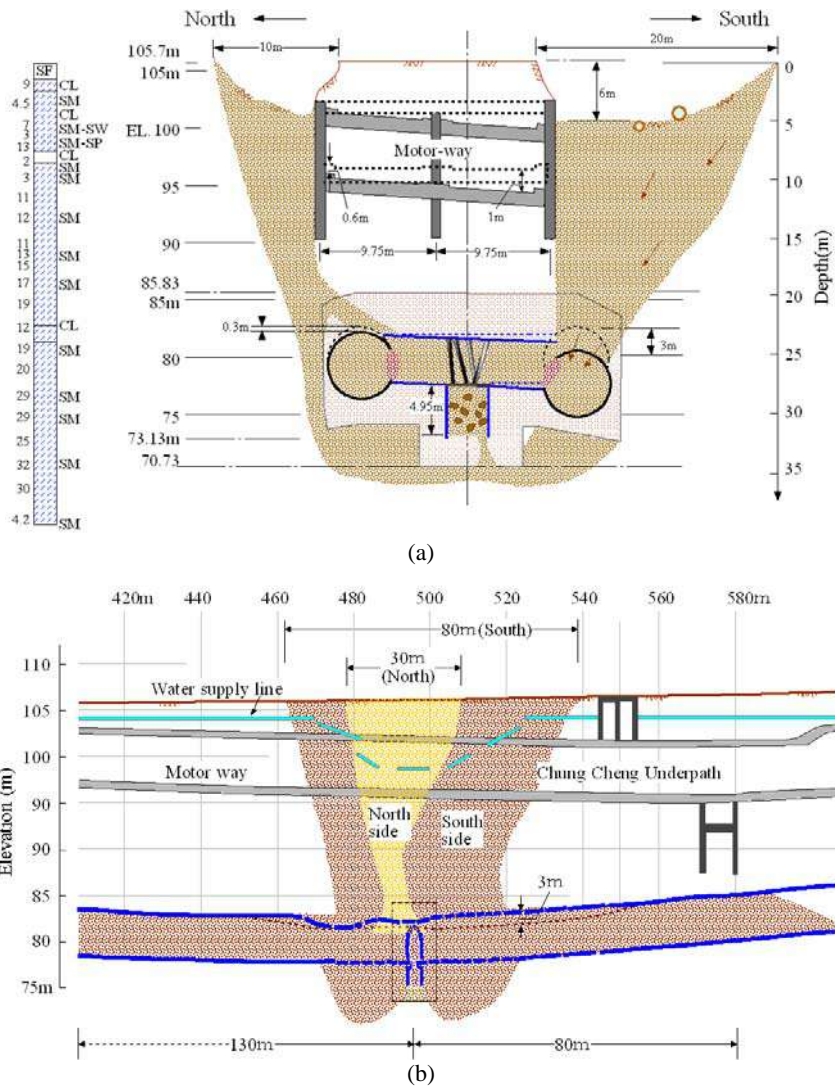


Figure 25 Failure scenario proposed, (a) cross sectional view, (b) longitudinal view (after Ishihara and Lee, 2008)



Figure 26 Wreckages of the crosspassage.

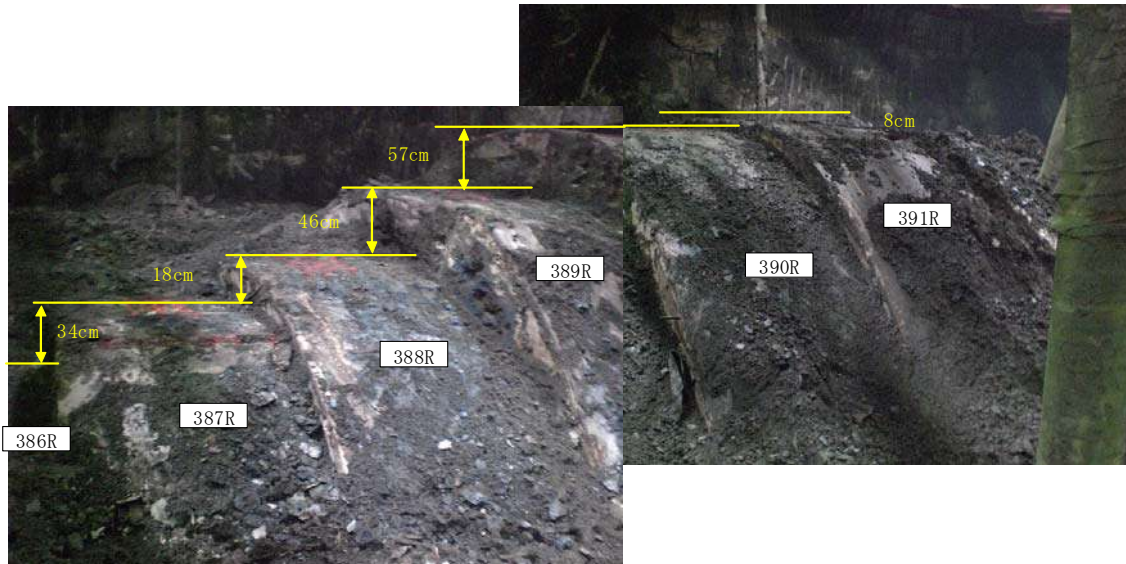


Figure 27 Damaged shield tunnel excavated during the retrofit works

A forensic investigation committee was formed to study the possible causes of failure. Comprehensive investigation and analysis were conducted including information presented in this paper. The reasons why such dreadful vertical cracks occurred at the bottom of the water sump were probably a combination of design layout, constructability, unique features of local soil, as well as quality control of ground improvement (TCRI, 2006). There were also some facts found that contributed to such massive ground failure. However, piping created by high hydraulic pressure and internal erosion prone local soil are believed to be the major causes of failure. Near 300kPa pressure difference between the constructed tunnel and the confining soil caused the collapse of water sump and led to even severe failure. The estimated seepage hydraulic gradient exceeded 12.5 (TCRI 2006; Ishihara and Lee, 2008).

7. CONCLUSIONS

This paper presents thorough information and deliberate investigation of a subway construction failure. Detailed time history of failure course was carefully documented. Specifically aimed testing methods, including borehole probing and 2D, 3D RIP tests, were also carried out to investigate the scope of the failure and to study the possible causes of failure. It was found that well documented site information at the time of accident and emergency works are most valuable to identify the possible failure scenario and thus organize the following up investigation. Both borehole probing test and RIP tests were found to be able to effectively understand the scope of failure and the condition of complicated underground environment. The failure scenario and failure causes would be clarified by summarizing these documented photos, records and forensic testing results. It is concluded that the studied accident was induced by unpredicted occurrence of piping in the non-plastic silty sand deposit subjected to a seepage field with fairly high hydraulic gradient.

The information presented in this paper is hoped to provide geotechnical engineers case references of similar forensic investigation, as well as precautions of similar construction works.

8. ACKNOWLEDGEMENT

The authors would like to thank Joint Venture MAEDA- Lung Dai, Kaohsiung Rapid Transit Company, Moh and Associates, and members of Forensic Investigation Committee for providing valuable information and instructive comments.

9. REFERENCES

- Chen, C. C. (2012), "Study on Engineering Properties of Low-Plasticity Silty Sand," doctoral dissertation, National Chen Kung University, Tainan, Taiwan, 266p
- Ishihara, K. and Lee, W. F. (2008), "Forensic diagnosis for site-specific ground conditions in deep excavations of subway constructions," Geotechnical and Geophysical Site Characterization, Proceeding of the 3rd International Conference on Site Characterization, Taipei, Taiwan, pp31-59.
- Lee, W. F., and Ishihara, K. (2008a), "Applications of Geophysics Methods in Underground Construction." Keynote paper, Applications of Innovative Technologies in Geotechnical Works, proceeding of The Hong Kong Institute of Engineers Geotechnical Division 28th Annual Seminar 2008, Hong Kong, China, page 23-34.
- Lee, W. F. and Ishihara, K. (2008b), "Immediate Retrofit Work and Forensic Investigation of A Subway Tunnel Construction Failure." Proceeding of 4th International Conference on Forensic Engineering - From Failure to Understanding, London, United Kingdom, page 259-268.
- TCRI, (2006), Forensic Investigation Report for KMRT LU009 Tunnel Failure (in Chinese).